A Forecast Evaluation of the North Pacific Jet Stream

David A. Lavers[1], Ryan D. Torn[2], David S. Richardson[1], Chris Davis[3], F. Martin Ralph[4], and Florian Pappenberger[1]

[1]European Centre for Medium-Range Weather Forecasts (ECMWF), Shinfield Park, Reading, RG2 9AX, U.K. [2]Department of Atmospheric and Environmental Science, University at Albany, State University of New York, Albany, New York, USA

[3]National Center for Atmospheric Research, Boulder, Colorado, USA. [4]Center for Western Weather and Water Extremes (CW3E), Scripps Institution of Oceanography, University of California, San Diego, La Jolla, California, USA

Aim

The aim of this study is to evaluate the North Pacific jet stream and its associated potential vorticity structure in the ECMWF Integrated Forecasting System (IFS).

Introduction

The jet stream generally refers to a narrow region of intense winds near the top of the troposphere. Along the jet stream, instabilities and waves can develop into midlatitude cyclones, which makes them critical for atmospheric predictability. Their key role in cyclogenesis also means they can be linked with atmospheric rivers, warm conveyor belts, and high-impact weather (e.g., extreme precipitation and winds). Given these impacts, it is important that numerical weather prediction (NWP) systems can accurately forecast the magnitude and the structure of jet streams.

Atmospheric River Reconnaissance (AR Recon)

The AR Recon campaign is a Research and Operations Partnership whose main aim is to help better inform decision-makers on water management and flooding in the western United States via the improvement of NWP forecasts (Ralph et al. 2020).

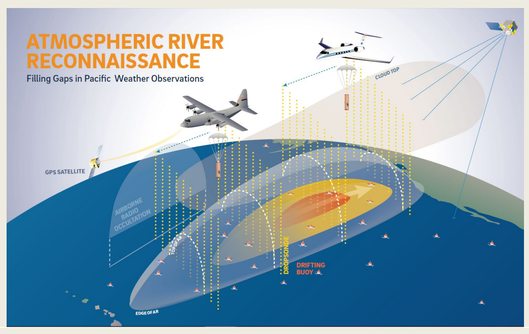

Fig. 1: Idealised AR Recon targeting concept (Zheng et al., 2021).

Research aircraft, such as the National Oceanic and Atmospheric Administration (NOAA) Gulfstream IV-SP (G-IV), use dropsondes to sample atmospheric rivers and other dynamically active regions, with the observations assimilated in real-time into global NWP systems, such as the ECMWF IFS, to improve the initialization of the next forecast. Observations gathered during AR Recon provide a unique opportunity to investigate the biases and the cross-jet structure of the North Pacific jet stream.

Data: observations and forecasts

During the 2020, 2021 and 2022 AR Recon seasons, the NOAA G-IV deployed 1,170 dropsondes and their locations are shown in Figure 2. This illustrates that a broad area of the northern Pacific was sampled.

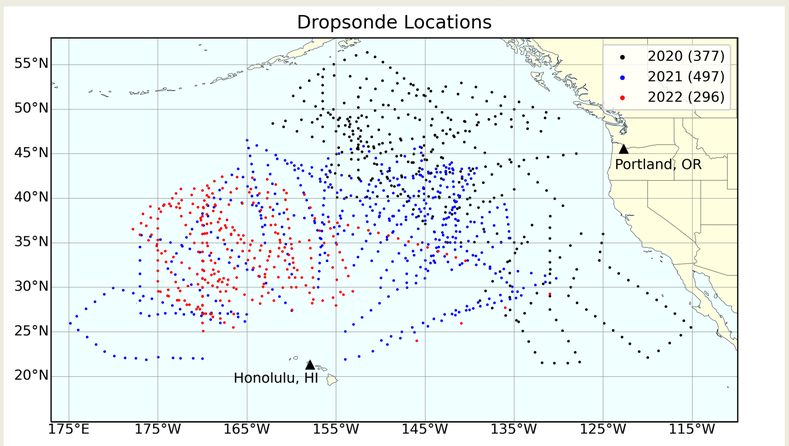

Fig. 2: The locations of the dropsondes deployed by the NOAA G-IV in 2020, 2021, and 2022. The NOAA G-IV was based in Portland, Oregon, in 2020, and in Honolulu, Hawaii, in 2021 and 2022. The number of dropsondes available in each year is given in the legend.

The long-window data assimilation (LWDA) system of the IFS consists of a 12-hour window where short-range (3-15 h) or background forecasts are combined with all observations (including the dropsonde data) via a four-dimensional variational data assimilation (4D-Var) process to produce a new LWDA analysis. The LWDA short-range forecasts and analyses are analysed here. It is the LWDA system that is used in the ECMWF IFS high-resolution forecast.

The high-resolution forecasts valid during 2020–2022 were interpolated from model levels on to a 20-hPa vertical resolution on a 0.1×0.1 regular grid. This evaluation considered forecasts from 0000 UTC for two and four days ahead (valid at the dropsonde time).

Methods and LWDA Results

The mean and standard deviation – which represent the mean and random errors, respectively – of the LWDA background-minus-observation (B-O) and analysis-minus-observation (A-O) departures are calculated in 20-hPa layers from 1000 hPa to 200 hPa using all assimilated pressure levels from the 1,170 dropsonde profiles. The results are shown in Figure 3.

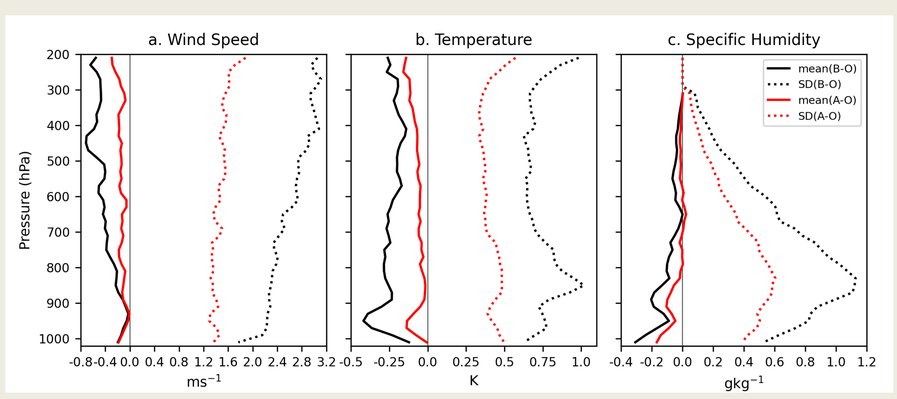

Fig. 3: The mean (solid lines) and standard deviation (dotted lines) of the background-minus-observation (B–O) and the analysis-minus-observation (A–O) departures (in the LWDA) in 20-hPa layers at the dropsonde locations for (a) wind speed, (b) temperature, and (c) specific humidity.

The structure of the jet stream is evaluated by considering transects of dropsonde profiles that cross the upper tropospheric jet at a relatively normal angle relative to the jet axis (no more than 30° to the jet axis). For the 2-d and 4-d forecasts, it is possible that the jet is not in the same geographic location as the observed jet at this time. This issue is addressed by shifting the forecast jet position to the observed jet position based on the difference in the "jet centroid" between the forecast and verifying analysis. Here the jet centroid is defined as the mass centroid of the 200-300 hPa layer-average wind within the jet.

The tropopause structure is assessed by computing the potential vorticity (PV) across the jet in the observations and model forecasts at the dropsonde locations.

Results

Figure 4 shows the relationship between the observed and model winds in the LWDA and high-resolution forecasts. These show (1) that the mean error, or bias, is negative which means that the model winds, on average, are weaker than the observed winds, and (2) as the lead time decreases, the model fit to the observations improves, as shown by the smaller standard deviation of the departures.

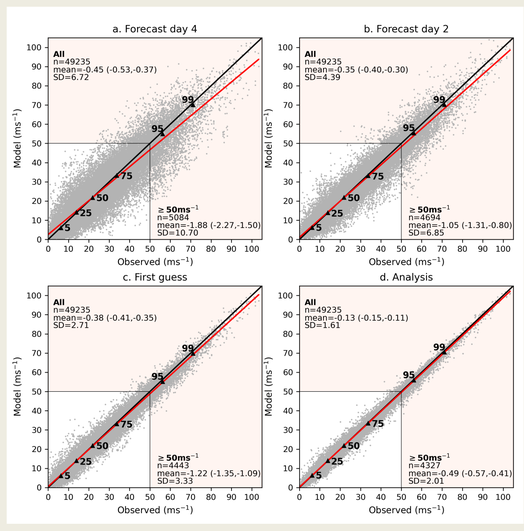

Fig. 4: Scatterplots of the observed versus model winds for (a) forecast day 4, (b) forecast day 2, (c) the LWDA background forecasts, and (d) the LWDA analysis in the 20-hPa resolution atmospheric profiles. In each panel, the sample size (n), and the mean and standard deviation of the forecast-minus-observation departures are given for all winds and for those ≥ 50 ms^{-1}. The 99 % confidence interval of the mean bias is also provided in the brackets. Red shaded regions represent winds ≥ 50 ms^{-1} (i.e., jet stream winds) and the 1:1 and linear regression lines are shown in black and red, respectively. Quantile-quantile points are also plotted as black triangles.

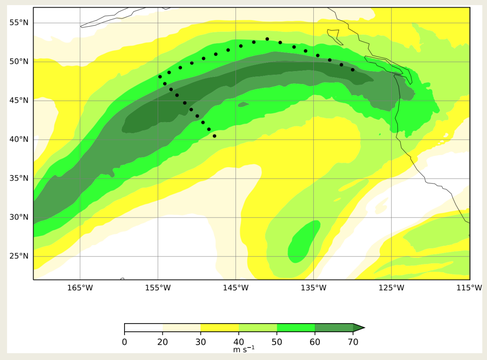

Fig. 5: An example Intensive Observing Period (IOP) on 15th February 2020

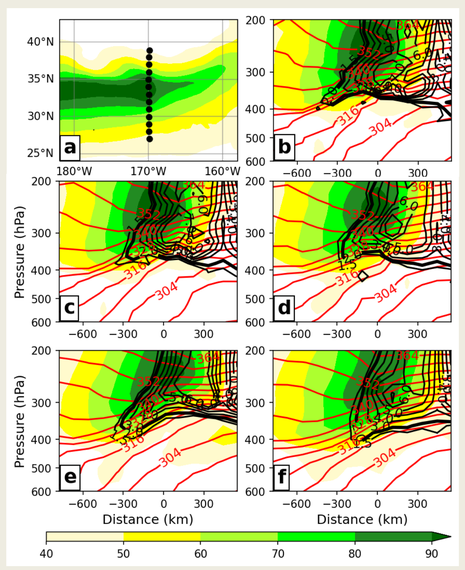

Fig. 6: An example intensive observing period (IOP) on 3rd February 2022. (a) The 250-hPa wind speed (shading) and the location of the dropsondes (black dots). Cross sections of the jet stream in the (b) observations, (c) analysis, (d) background, (e) forecast day 2, and (f) forecast day 4. In panels (b–f), the wind speed is shown as shading, the PV is given by black contours, and the potential temperature is shown by red contours. Note that the north is on the right-hand side of the cross sections, so that the wind is coming out of the page, and the x-axis shows the distance relative to the maximum jet stream wind.

Example transects are presented in Figures 5 and 6. The PV is shown across the jet on 3rd February 2022 (Fig. 6) and the observations have an upper-level front (Fig. 6b). There is evidence that, at times, the IFS cannot capture the PV gradient across the tropopause (e.g., Fig. 6d and Fig. 6f).

Results

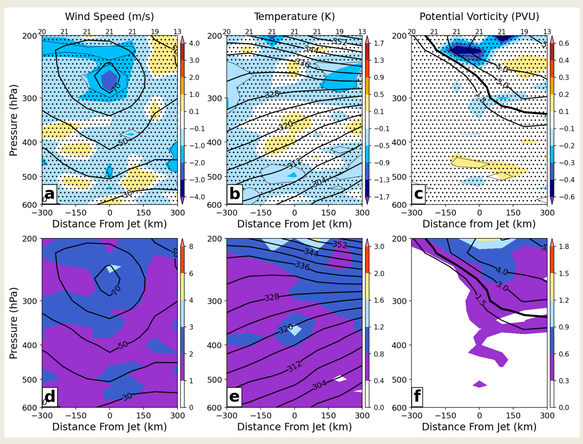

Fig. 7: Cross sections of the jet stream in the background forecasts using the 20-hPa resolution atmospheric profiles. The composite mean bias (a–c) and mean absolute error (d–f) of the wind speed, potential temperature, and PV are shown as shaded colours and the mean observations are shown as line contours. Note that the north is on the right-hand side of the cross sections, so that the wind is coming out of the page. The x-axis shows the distance relative to the maximum jet stream wind, and the numbers along the top of panels (a–c) signify the number of dropsonde profiles used in the composite at those locations. (a–c) Stippling shows non-significant areas at the 95 % level.

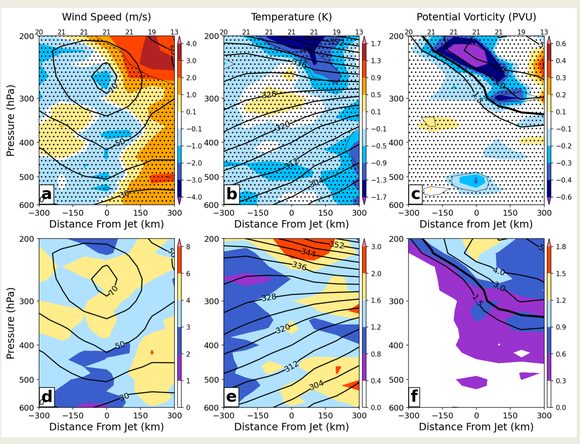

Fig. 8: Same as Fig. 7, but for forecast day 2.

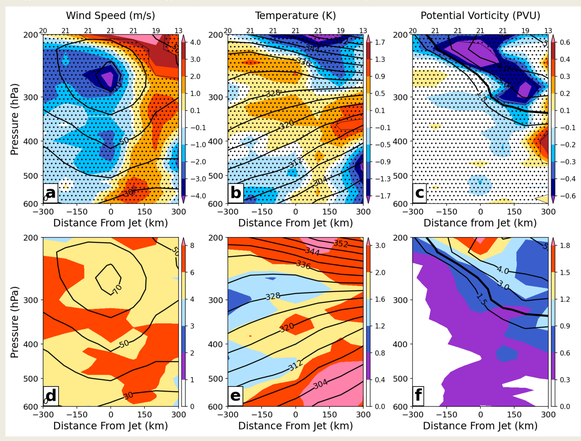

Fig. 9: Same as Fig. 7, but for forecast day 4.

Results show that the PV gradient across the tropopause weakens with lead time (Fig. 7c, 8c, 9c) meaning that the sharp gradients across the tropopause are diffused away. A statistically significant slow wind bias is found in the jet in the background and on day 4 (Fig. 7a, 9a).

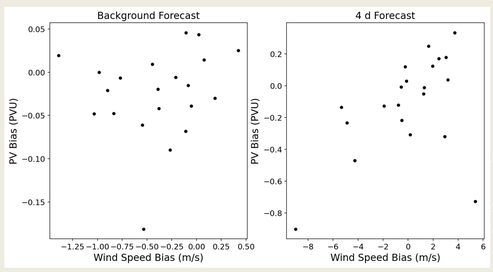

Fig. 10 (left): Scatterplots of wind speed bias versus PV bias in the background and on day 4.

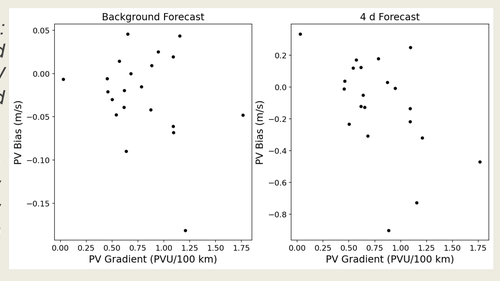

Fig. 11 (right): Scatterplots of the PV gradient versus PV bias in the background and on day 4.

Discussion

There are two aspects of the current ECMWF IFS configuration that might be responsible for the too weak a PV gradient across the tropopause. The first possible issue is the vertical resolution of the model levels in the upper troposphere and lower stratosphere (UTLS). The second factor is the value of vertical diffusion coefficients applied in the UTLS.

Based on these results, experiments are now being planned to test a higher vertical resolution to determine if this will provide a more skillful simulation of the UTLS and jet stream in the IOPs studied here.

As the PV gradient near the tropopause is important for Rossby wave propagation, an improvement in modelling the UTLS may lead to increased forecast skill.

Further Reading

Ralph, F. M. et al. 2020: West Coast Forecast Challenges and Development of Atmospheric River Reconnaissance. *Bull. Amer. Meteor. Soc.,* 101, E1357–E1377.

Zheng, M. et al. 2021: Data gaps within atmospheric rivers over the northeastern Pacific. Bulletin of the American Meteorological Society, 102(3), pp.E492-E524.